Large-Signal Stability Analysis of Self-Turn-On in Switching Transients

Wen Zhang
Min H. Kao Dept. of EECS
The University of Tennessee
Knoxville, USA
wen.zhang@utk.edu

Fred Wang
Min H. Kao Dept. of EECS
The University of Tennessee
Oak Ridge National Lab.
Knoxville, USA
fred.wang@utk.edu

***Abstract*—Unstable switching transient oscillation can be detrimental or destructive to power electronics converters. As switching speed increases, the impact of parasitic components became more severe and may lead to unexpected switching behavior. The large-signal and nonlinear nature of the switching transients limits the use of small-signal analysis where operating points must be carefully selected. The Lyapunov function based on Brayton-Moser's mixed potential method is applied here to analyze the self-turn-on phenomena in MOSFETs' turn-off transient. It is shown that the switching transient can be expressed as a gradient descent of a mixed potential function. The large-signal stability theorem provides a metric to quantitatively evaluate the switching transient stability. Comparison with the experimental results shows it can effectively predict the significance of the unstable oscillation and explain the root cause of the self-turn-on phenomena.**

***Index Terms*—Switching transient; large-signal stability; parasitic inductance; parasitic capacitance; power semiconductor**

I. Introduction

As the switching speed of power semiconductors increases, especially with the advent of wide-bandgap devices, the switching transient becomes very sensitive to the parasitic elements. In addition to more severe switching transient oscillation, unwanted oscillation pattern or even instability may occur. It is shown a moderate amount of common source inductance can induce significant self-turn-on phenomena in Si CoolMOS [1]. The MOSFET channel is falsely turned back on momentarily during its turn-off transient, where the voltage across the common source inductance charges the gate-source capacitance above the threshold voltage. In the worst case, the oscillation is sustainable and the switching control over the MOSFET is completely lost. Similar phenomena where the device failed to turn off have been observed in GaN HEMT in cryogenic temperatures, supposedly with much smaller common source inductance [2].

The power semiconductor switching transient stability is studied in several previous works. The unstable switching due to gate-drain capacitance C_{gd} feedback has been reported in [3]. Similar phenomena have been discussed with oscillator theory in [4]. Optimizing both the gate-drain capacitance C_{gd} and common source inductance L_s to mitigate the unwanted oscillation is presented in [5]. However, the aforementioned approaches leverage the small-signal model and analysis which requires careful selection of operating points.

A large-signal analysis approach based on Lyapunov function for electrical networks was proposed in [6] by Brayton and Moser. The large-signal stability can be analyzed by evaluating the properties of the mixed potential function. In this paper, large-signal stability analysis with Brayton-Moser's mixed potential function is presented. The mixed potential function is first formulated, and then the relationship between the system trajectory and the mixed potential function is shown. Finally, the large-signal stability theorem is applied to the self-turn-on scenarios to illustrate the relationship between a characteristic value $\mu_1 + \mu_2$ and the severity of the unwanted oscillation.

II. Brayton-Moser's Mixed Potential

Lyapunov's direct method provides a framework for analyzing the stability of nonlinear systems, and it relies on constructing a potential function $P(\boldsymbol{x})$, or Lyapunov function [7]. Constructing the potential function $P(\boldsymbol{x})$ is generally is difficult. Brayton-Moser's mixed potential method is a systematical method to construct such a function for electrical networks [6]. The mixed potential function $P(\boldsymbol{x}) = P(\boldsymbol{i}, \boldsymbol{v})$ has the unit of power and has the following general form, where $A(\boldsymbol{i})$ is the terms related to the independent current vector $\boldsymbol{i}$, $B(\boldsymbol{v})$ is the terms related to the independent voltage vector $\boldsymbol{v}$, and $N(\boldsymbol{i}, \boldsymbol{v})$ is the terms related to both the current and voltage vectors.

$$P(\boldsymbol{i}, \boldsymbol{v}) = A(\boldsymbol{i}) - B(\boldsymbol{v}) + N(\boldsymbol{i}, \boldsymbol{v}). \tag{1}$$

The equivalent circuit of the switching transient is shown in Fig. 1(a). During the switching transient, the MOSFET stayed in ohmic region before the gate-source voltage v_{gs} is being discharged below the Miller voltage $V_{th} + \frac{I_L}{g_{fs}}$. The drain-source voltage v_{ds} only starts to change after the MOSFET goes into saturation region. Therefore, the period in the ohmic region can be neglected. The MOSFET channel current in saturation region and cut-off region can be modeled by a voltage controlled current source,

$$i_M(v_{gs}) = \begin{cases} 0, & \text{if } v_{gs} < V_{th}, \\ g_{fs}(v_{gs} - V_{th}), & \text{otherwise.} \end{cases} \tag{2}$$

The diode model here assumes a forward voltage $V_f = 0$, a forward resistance of $R_f \neq 0$ and a voltage-dependent

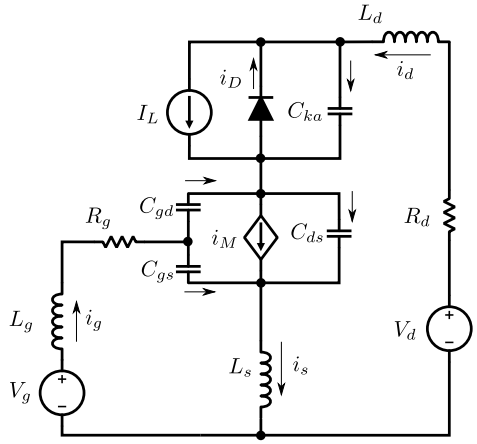

(a) Phase leg switching transient circuit model.

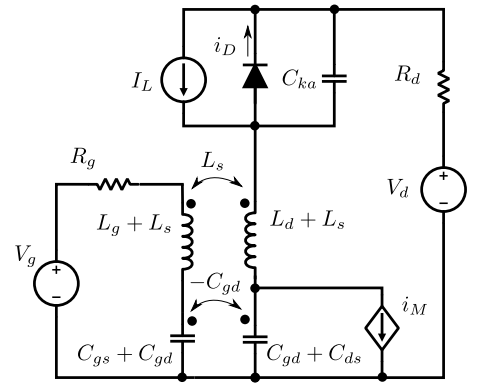

(b) Phase leg equivalent circuit with coupling terms.

Fig. 1. Switching transient circuit model: (a) phase leg circuit model with parasitic elements; (b) equivalent circuit model with coupling terms.

parasitic capacitance C_{ka}. The diode current i_D going through its junction can be written as,

$$i_D(v_{ka}) = \begin{cases} 0, & \text{if } v_{ka} > 0, \\ -R_f^{-1} v_{ka}, & \text{otherwise.} \end{cases} \tag{3}$$

From the circuit in Fig. 1(a), we can easily see that $i_g + i_d = i_s$ and $v_{gs} = v_{gd} + v_{ds}$. Therefore, the independent variables of the circuit are selected to be $\boldsymbol{x} = [\boldsymbol{i}\ \boldsymbol{v}]^T$, $\boldsymbol{i} = [i_g\ i_d]^T$, and $\boldsymbol{v} = [v_{gs}\ v_{ds}\ v_{ka}]^T$. Because i_s and v_{gd} are dependent variables, the remaining gate-drain capacitance C_{gd} and common-source inductance L_s in Fig. 1(a) are substituted with coupling terms to facilitate the mixed potential function formulation. The equivalent circuit with the coupling elements is shown in Fig. 1(b).

The first step to formulate the mixed potential function is to construct the current potential for the voltage sources and current-controlled resistors, and voltage potential for the voltage-controlled resistors and current sources [8]. The voltage potential of the MOSFET channel in the saturation region can be represented as a pseudo-resistor [9],

$$\frac{1}{2} G_M v_{ds}^2, \tag{4}$$

where $G_M = g_{fs}(v_{gs} - V_{th})/v_{ds}$ when $v_{gs} > V_{th}$, and $G_M = 0$ otherwise.

The voltage potential of the diode current i_D can also be represented as a pseudo-resistor,

$$\frac{1}{2} G_D v_{ka}^2, \tag{5}$$

where $G_D = R_f^{-1}$ when $v_{ka} \le 0$, and $G_D = 0$ otherwise.

The current or voltage potential of the other elements such as the voltage source and capacitors in the circuit Fig. 1(b) can be easily obtained from [6]. Finally, the mixed potential function is given by summing them together,

$$\begin{aligned} P = &- V_g i_g - V_d i_d - I_L v_{ka} \\ &+ \frac{1}{2} R_g i_g^2 + \frac{1}{2} R_d i_d^2 \\ &- \frac{1}{2} G_M v_{ds}^2 - \frac{1}{2} G_D v_{ka}^2 \\ &+ v_{ds} i_d + v_{gs} i_g + v_{ka} i_d. \end{aligned} \tag{6}$$

Rewriting it in the standard form in (1),

$$A(\boldsymbol{i}) = -V_g i_g - V_d i_d + \frac{1}{2} R_g i_g^2 + \frac{1}{2} R_d i_d^2, \tag{7}$$

$$B(\boldsymbol{v}) = I_L v_{ka} + \frac{1}{2} G_M v_{ds}^2 + \frac{1}{2} G_D v_{ka}^2, \tag{8}$$

$$N(\boldsymbol{i}, \boldsymbol{v}) = v_{ds} i_d + v_{gs} i_g + v_{ka} i_d. \tag{9}$$

Thus, the mixed potential function or the Lyapunov function for the switching transient circuit is derived. Note the functions G_M and G_D are directly related to the static characteristics of the MOSFET and diode. Although relatively simple equations are used to describe their characteristics, more complex ones can be easily plugged in to better describe the circuit. If using numerical computations, piece-wise-linear or more complex regression functions can be used [10].

III. Switching Transient Trajectory

Given $\boldsymbol{x} = [\boldsymbol{i}\ \boldsymbol{v}]^T$, $\boldsymbol{i} = [i_g\ i_d]^T$, and $\boldsymbol{v} = [v_{gs}\ v_{ds}\ v_{ka}]^T$, the validity of the mixed potential function in (6) can be easily verified because the mixed potential function $P(\boldsymbol{x})$ describes the system trajectory by satisfying the equation below [6].

$$\begin{bmatrix} -L(\boldsymbol{i}) & 0 \\ 0 & C(\boldsymbol{v}) \end{bmatrix} \frac{d\boldsymbol{x}}{dt} = Q(\boldsymbol{x}) \frac{d\boldsymbol{x}}{dt} = \frac{dP}{d\boldsymbol{x}}, \tag{10}$$

where the inductance and capacitance matrices are given by

$$L(\boldsymbol{i}) = \begin{bmatrix} L_g + L_s & L_s \\ L_s & L_d + L_s \end{bmatrix}, \tag{11}$$

$$C(\boldsymbol{v}) = \begin{bmatrix} C_{gs} + C_{gd} & -C_{gd} & 0 \\ -C_{gd} & C_{gd} + C_{ds} & 0 \\ 0 & 0 & C_{ka} \end{bmatrix}, \tag{12}$$

$$Q(\boldsymbol{x}) = \begin{bmatrix} -L(\boldsymbol{i}) & 0 \\ 0 & C(\boldsymbol{v}) \end{bmatrix}. \tag{13}$$

Note the capacitances $C_{gs},\ C_{gd},\ C_{ds}$ and C_{ka} are typically nonlinear and voltage-dependent for power semiconductor devices. So the capacitance matrix $C(\boldsymbol{v})$ is voltage dependent. The inductances $L_g,\ L_d$ and L_s are due to the magnetic flux of

TABLE I. Modeling parameters

Parameter	Value
MOSFET	IXKR47N60C5
Diode	C4D20120D
L_g	10.0 nH
L_d	20.0 nH
L_s	4.0 nH

the PCB trace or semiconductor packaging. They are usually constant and not current-dependent. Therefore, the inductance matrix $L(\boldsymbol{i}) = L$ is a constant matrix.

We can immediately see that (10) completely describes the switching transient circuit system. The steady-state operating point of the circuit can be trivially found by solving $\frac{dP}{d\boldsymbol{x}} = 0$. Moving $Q(\boldsymbol{x})$ to the right,

$$\frac{d\boldsymbol{x}}{dt} = Q^{-1}(\boldsymbol{x})\frac{dP}{d\boldsymbol{x}}. \tag{14}$$

It is obvious that the gradient of every point $\boldsymbol{x}$ on the system trajectory is given by $Q^{-1}\frac{dP}{d\boldsymbol{x}}$, which means the system trajectory is directly related to the product of the gradient of the mixed potential function $P(\boldsymbol{x})$ and the inverse of the passive element matrix $Q(\boldsymbol{x})$.

So far, it is shown that there is a direct relationship between the mixed potential function and the system trajectory. To help illustrate the relationship between the time-domain system trajectory and the mixed potential function, time-domain simulation is performed by solving (10), and the mixed potential function is plotted against time. The parasitic elements and switching devices in the model are from [1] and listed in Table I if not mentioned otherwise.

Three cases where only the load current I_L is different are simulated and there switching transient waveforms are plotted along with its mixed potential function $P(\boldsymbol{x})$. In all three cases, the DC link voltage is 200 V and the gate resistance is 2.0 Ω. The load current I_L is varied between 5 A, 15 A and 30 A. The self-turn-on phenomenon worsens with higher load current, with the switching transient waveforms appear more oscillatory and abnormal with increasing load current I_L. Specifically, the self-turn-on phenomena become self-sustained and the MOSFET fails to be turned off when the load current is 30 A, coinciding with the experimental result [1]. The mixed potential function shows similar trend where it becomes more oscillatory with higher load current. During the turn-off transient, the mixed potential when $I_L = 5\ A$ drops down to zero with very little oscillation. In the worst case when $I_L = 30\ A$, the mixed potential keeps oscillating seemingly forever.

IV. Switching Transient Large-Signal Stability

A. Asymptotic Stability Criteria

What is more interesting to us is whether it is possible to predict the stability of the system without performing the time-domain simulation. As shown in (10), the system trajectory is completely described by $P(\boldsymbol{x})$ and $Q(\boldsymbol{x})$. This means it is potentially feasible to evaluate a system's stability by only

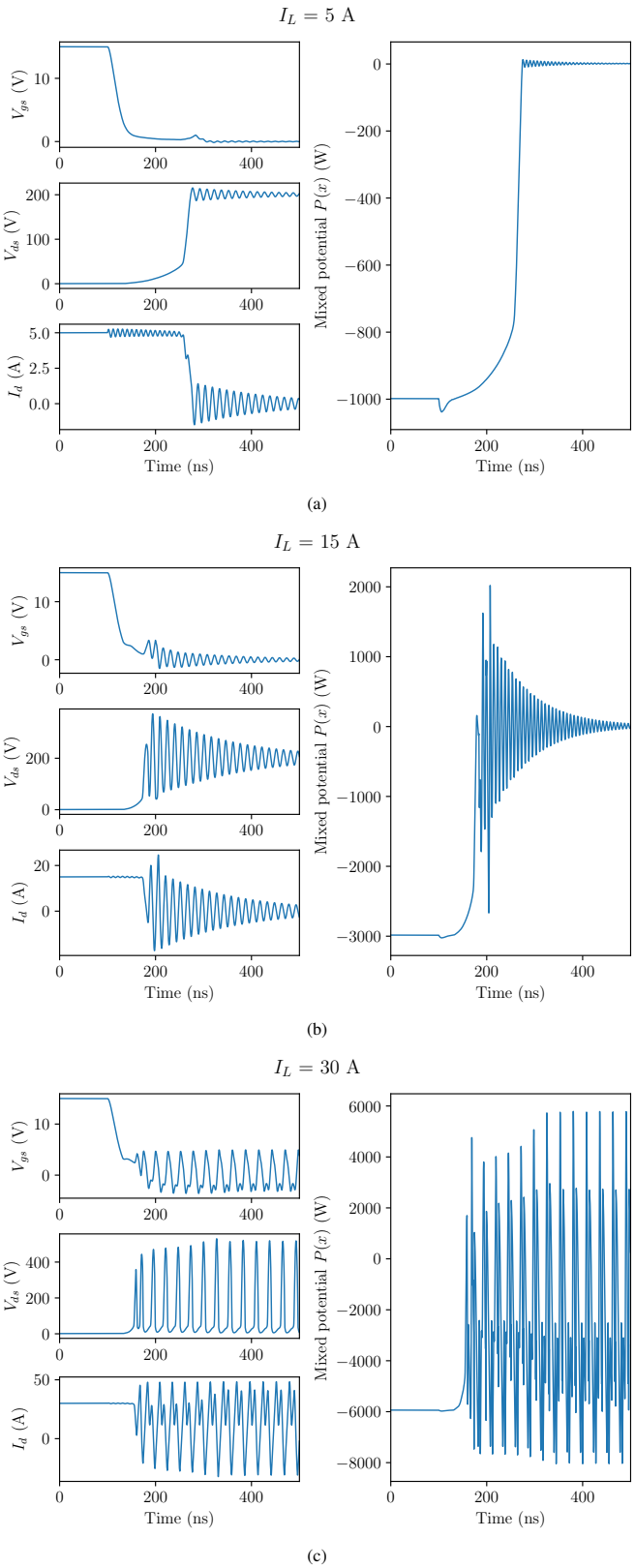

Fig. 2. Simulated turn-off switching transient waveforms with self-turn-on phenomena and the corresponding mixed potential function at 200 V DC link voltage and 2.0 Ohm gate resistance: (a) 5 A; (b) 15 A; (c) 30 A.

looking at $P(\boldsymbol{x})$ and $Q(\boldsymbol{x})$, which is the general concept of Lyapunov's direct method.

While [6] provides several theorems to predict the system stability, the theorems require some strict linearity properties of the passive component matrix $Q(\boldsymbol{x})$ or the interconnection function $N(\boldsymbol{x})$. A more general stability theorem is proposed in [8], where the asymptotic stability can be then evaluated by calculating some characteristic value, the infimum of the eigenvalues of some intermediate matrices. First let

$$K_1(\boldsymbol{i},\boldsymbol{v}) = \frac{1}{2}A_{ii}(\boldsymbol{i}) + \frac{1}{2}\left([A_i(\boldsymbol{i}) + \gamma\boldsymbol{v}]^T L^{-1}(\boldsymbol{i})\right)_i L(\boldsymbol{i}),$$
$$K_2(\boldsymbol{i},\boldsymbol{v}) = \frac{1}{2}B_{vv}(\boldsymbol{i}) + \frac{1}{2}\left([B_v(\boldsymbol{v}) - \gamma^T\boldsymbol{i}]^T C^{-1}(\boldsymbol{v})\right)_v C(\boldsymbol{v}).$$

Note the subscript here means derivative. For example, $A_{ii}(\boldsymbol{i})$ means the second-order derivative of the function $A(\boldsymbol{i})$ against the independent current vector $\boldsymbol{i}$. Let

$$K_j^s(\boldsymbol{x}) = \frac{1}{2}\left(K_j(\boldsymbol{x}) + K_j^T(\boldsymbol{x})\right),$$

where $j = 1, 2$ denote their corresponding symmetric parts. Furthermore, also define

$$\widetilde{K}_1^s(\boldsymbol{i},\boldsymbol{v}) = L^{-\frac{1}{2}}(\boldsymbol{i})K_1^s(\boldsymbol{i},\boldsymbol{v})L^{-\frac{1}{2}}(\boldsymbol{i}),$$
$$\widetilde{K}_2^s(\boldsymbol{i},\boldsymbol{v}) = C^{-\frac{1}{2}}(\boldsymbol{v})K_2^s(\boldsymbol{i},\boldsymbol{v})C^{-\frac{1}{2}}(\boldsymbol{v}).$$

Suppose $\delta_S(x) = \{\delta_1(x), \delta_2(x), \cdots, \delta_m(x)\}$ is the set of eigenvalues for a symmetric set $S(x)$, let $\mu(S)$ denote the infimum of the eigenvalues of $S(x)$ over all x,

$$\mu(S) = \inf\{\delta(x)\}.$$

Finally, denote

$$\mu_1 = \mu(\widetilde{K}_1^s),$$
$$\mu_2 = \mu(\widetilde{K}_2^s).$$

The sufficient but not necessary condition for asymptotic stability is

$$\mu_1 + \mu_2 \geq \delta,\ \delta > 0, \tag{15}$$

and $P^\star(\boldsymbol{x}) \to \infty,$ as $|\boldsymbol{x}| \to \infty$.

Note that asymptotic stability is a very "strong" stability requirement where all points around the equilibrium point are drawn toward it and will reach the equilibrium point as time goes infinity. In practice, the theorem may not suffice even though the switching transient appears normal. More discussions will be provided in the case studies and parametric studies below.

B. Switching Transient Stability

From previous standard form, the following first order derivatives can be easily obtained.

$$A_i(\boldsymbol{i}) = \begin{bmatrix} -V_g + R_g i_g \\ -V_d + R_d i_d \end{bmatrix},$$
$$B_v(\boldsymbol{v}) = \begin{bmatrix} 0 \\ G_M v_{ds} \\ I_L + G_D v_{ka} \end{bmatrix}.$$

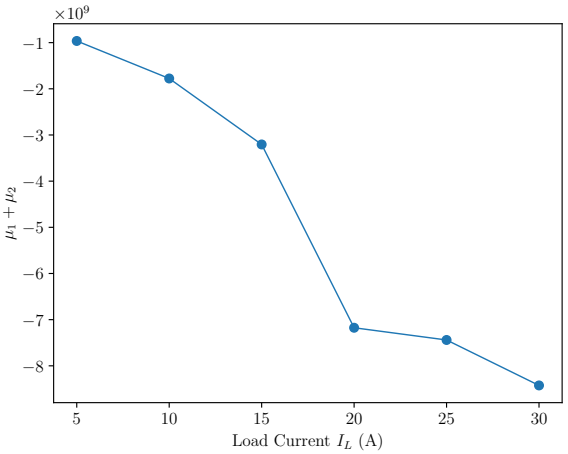

Fig. 3. Value of $\mu_1 + \mu_2$ for different load current I_L with 200 V DC link voltage and 2.0 Ω gate resistance.

The second order derivatives can then be derived.

$$A_{ii}(\boldsymbol{i}) = \begin{bmatrix} R_g & 0 \\ 0 & R_d \end{bmatrix},$$
$$B_{vv}(\boldsymbol{v}) = \begin{bmatrix} 0 & 0 & 0 \\ 0 & G_M & 0 \\ 0 & 0 & G_D \end{bmatrix}.$$

The interconnection matrix is given by

$$\gamma = \begin{bmatrix} 1 & 0 & 0 \\ 0 & 1 & 1 \end{bmatrix}.$$

Furthermore, because in the switching transient $L(\boldsymbol{i}) = L$ is a constant matrix, $K_1(x)$ can be simplified,

$$K_1(\boldsymbol{i},\boldsymbol{v}) = \frac{1}{2}A_{ii}(\boldsymbol{i}) + \frac{1}{2}([A_i(\boldsymbol{i}) + \gamma\boldsymbol{v}]^T)_i = A_{ii}(\boldsymbol{i}).$$

However, the capacitance matrix $C(\boldsymbol{v})$ is indeed voltage dependent. Therefore, $K_2(\boldsymbol{x})$ is more complex and has to be calculated numerically, which can be readily done in numerical computation software.

V. Parametric Study on Self-Turn-On Phenomena

As shown in Fig. 2, the self-turn-on phenomena become worse with higher load current and complete instability occurs when the load current reaches 30 A. The value of $\mu_1 + \mu_2$ is calculated for different load current conditions but with the same 200 V DC voltage and 2.0 Ω gate resistance and plotted in Fig. 3. The significance of the self-turn-on phenomena coincides with the values of $\mu_1 + \mu_2$, where it is more negative when the phenomenon is worse. Compared to the case where $I_L = 5\ A$, the value in the $I_L = 30A$ case is much smaller.

Similarly, the gate resistance R_g is varied while the load current I_L is kept at 20 A. In the experimental results in [1], it is found that the worst self-turn-on happens not with the smallest gate resistance nor with the largest, but somewhere in between. This is also observed in evaluating $\mu_1 + \mu_2$. The

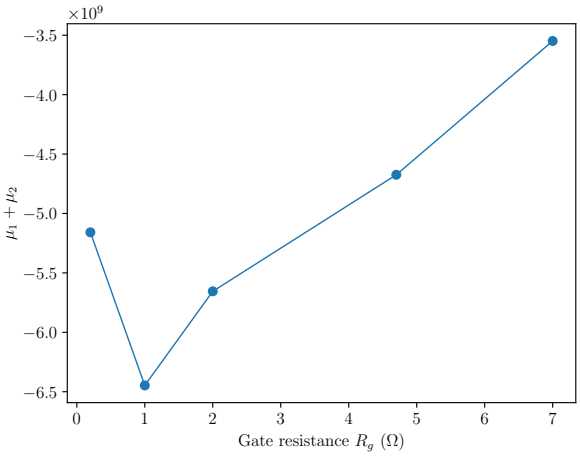

Fig. 4. Value of $\mu_1 + \mu_2$ for different gate resistance R_g with 200 V DC link voltage, 20 A load current.

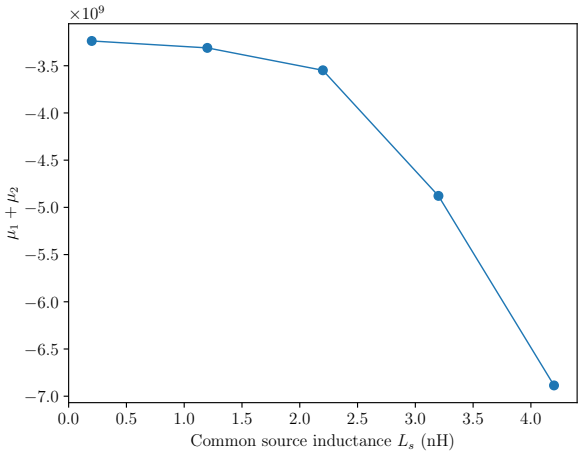

Fig. 6. Value of $\mu_1 + \mu_2$ for different common source inductance L_s with 200 V DC link voltage, 20 A load current and 2.0 Ω gate resistance.

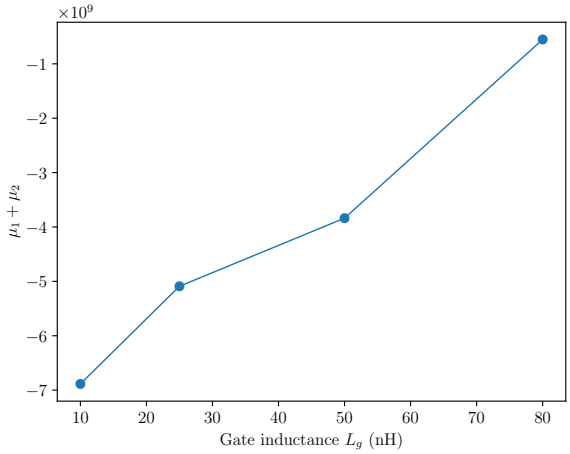

Fig. 5. Value of $\mu_1 + \mu_2$ for different gate inductance L_g with 200 V DC link voltage, 15 A load current and 4.7 Ω gate resistance.

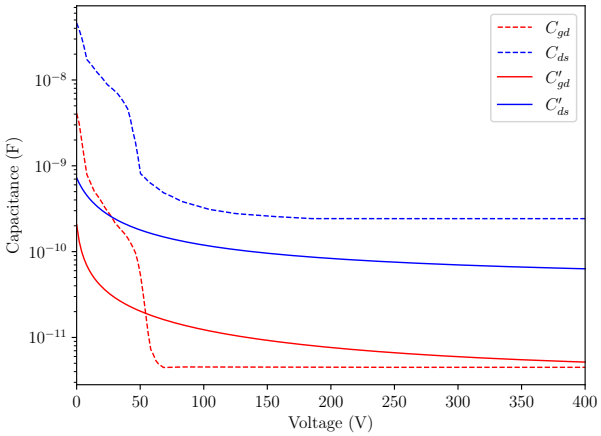

Fig. 7. Capacitance-votlage curve of CoolMOS IXKR47N60C5 (dashed) and Wolfspeed C3M0065090D (solid).

smallest value of $\mu_1 + \mu_2$ happens when $R_g = 2.0\ \Omega$ instead of the smallest or the largest gate resistance.

A potential approach to mitigate the self-turn-on phenomena is to increase the gate inductance [11]. Similarly, the gate inductance L_g is varied and $\mu_1+\mu_2$ is calculated at each point, and the result is shown in Fig. 5. The DC link voltage is kept at 200 V, gate resistance at 4.7 Ω and the load current at 15 A. The trend shows the self-turn-on phenomena is significantly alleviated when the gate inductance is larger, which coincides with the results in [11]. This means the theorem or the method here can be applied to optimize the gate driver design.

Finally, the common-source inductance L_s is varied to understand its contribution in the stability criteria, and it is shown in Fig. 6. It is clearly seen that smaller common source inductance helps increasing the value of $\mu_1 + \mu_2$.

However, although the value $\mu_1 + \mu_2$ clearly shows relationship with the significance of the instability, the value $\mu_1 + \mu_2$ is still negative while the self-turn-on phenomena in some of the previous cases may be already insignificant or even nonexistent. The asymptotic stability theorem is still not satisfied. This is because of another root cause of the self-turn-on phenomena, the unconventional capacitance-voltage curve of the CoolMOS, as shown in Fig. 7. The parasitic capacitance of IXKR47N60C5 changes drastically at around 50 V. Intuitively, the drastic change in capacitance means a sharp increase in voltage slew rate during the turn-off transient, and the current in the MOSFET channel is effectively dumped into the parasitic capacitance, inciting a potential instability.

To understand the contribution of the capacitance-voltage curve to the instability, the capacitances of the device is hypothetically changed to those of Wolfspeed C3M0065090D. Given C3M0065090D is a SiC MOSFET with comparable current rating and smaller parasitic capacitance, the switching speed is much faster than IXKR47N60C5. However, the

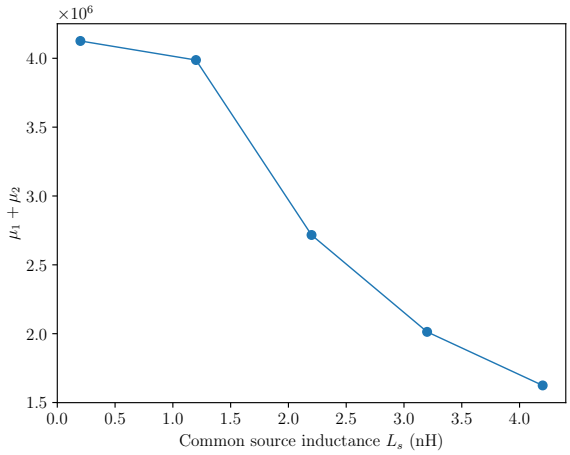

Fig. 8. Value of $\mu_1 + \mu_2$ for different common source inductance L_s with 200 V DC link voltage, 20 A load current 2.0 Ω gate resistance, and the capacitances of C3M0065090D.

calculated $\mu_1 + \mu_2$ is positive with otherwise same parameters. The sweep of the common-source inductance is shown in Fig. 8. Therefore, the other cause of the instability being the capacitance-voltage curve is verified. Looking back at $K_2(\boldsymbol{x})$, the derivative term associated with $C^{-1}(\boldsymbol{v})$ clearly indicates the capacitance-voltage dependence plays a role in the overall stability, which is typically not considered in small-signal analysis.

In conclusion, the characteristic value of $\mu_1 + \mu_2$ is an indication of the severity of the self-turn-on phenomena and can be used to predict its occurrence or to help with the gate driver design.

VI. Conclusions

Switching transients are highly nonlinear and large-signal by their nature. Large-signal analysis theory by Brayton and Moser is applied here and the mixed potential function is derived. It is shown there is a direct relationship between the time-domain system trajectory and the mixed potential function. The analytical result from the theorem coincides with the phenomena observed in experiments, indicating that it can predict the stability and help with circuit design. Parametric study on circuit parasitic elements shows the major contributors to the self-turn-on phenomena are the common-source inductance and the CoolMOS's unconventional capacitance-voltage curve. It is also observed that the theorem is conservative, where the asymptotic stability criterion is violated although the self-turn-on phenomenon is insignificant. A interesting question and future work may be whether it is possible to define a margin within which a negative characteristic value is tolerable.

Acknowledgment

This work made use of Engineering Research Center shared facilities supported by the Engineering Center Program of the National Science Foundation and the Department of Energy under NSF Award Number EEC-1041877 and the CURENT Industry Partnership Program.

References

[1] W. Zhang, Z. Zhang, F. Wang, D. Costinett, L. Tolbert, and B. Blalock, "Common source inductance introduced self-turn-on in MOSFET turn-off transient," in *Conference Proceedings - IEEE Applied Power Electronics Conference and Exposition - APEC*, IEEE, 2017, pp. 837–842.

[2] R. Ren, H. Gui, Z. Zhang, R. Chen, J. Niu, F. Wang, L. M. Tolbert, B. J. Blalock, D. J. Costinett, and B. B. Choi, "Characterization of 650 v Enhancement-mode GaN HEMT at Cryogenic Temperatures," *2018 IEEE Energy Conversion Congress and Exposition, ECCE 2018*, pp. 891–897, 2018.

[3] D. A. Grant and J. Gowar, *Power MOSFETs: theory and applications*. Wiley-Interscience, 1989.

[4] A. Lemmon, M. Mazzola, J. Gafford, and C. Parker, "Instability in half-bridge circuits switched with wide band-gap transistors," *IEEE Transactions on Power Electronics*, vol. 29, no. 5, pp. 2380–2392, 2014.

[5] R. Matsumoto, K. Umetani, and E. Hiraki, "Optimization of the balance between the gate-Drain capacitance and the common source inductance for preventing the oscillatory false triggering of fast switching GaN- FETs," *2017 IEEE Energy Conversion Congress and Exposition, ECCE 2017*, vol. 2017-Janua, pp. 405–412, 2017.

[6] R. K. Brayton and J. K. Moser, "A theory of nonlinear networks. I," *Quarterly of Applied Mathematics*, vol. 22, no. 1, pp. 1–33, 1964.

[7] J. Slotine and W. Li, *Applied Nonlinear Control*. Prentice hall Englewood Cliffs, NJ, 1990.

[8] D. Jeltsema and J. M. Scherpen, "On Brayton and Moser's Missing Stability Theorem," *IEEE Transactions on Circuits and Systems II: Express Briefs*, vol. 52, no. 9, pp. 550–552, 2005.

[9] B. E. Shi, "Pseudoresistive networks and the pseudovoltage-based cocontent," *IEEE Transactions on Circuits and Systems I: Fundamental Theory and Applications*, vol. 50, no. 1, pp. 56–64, 2003.

[10] W. Zhang, Z. Zhang, F. Wang, D. Costinett, L. M. Tolbert, and B. J. Blalock, "Characterization and Modeling of a SiC MOSFET's Turn-On Overvoltage," *2018 IEEE Energy Conversion Congress and Exposition, ECCE 2018*, pp. 7003–7009, 2018.

[11] B. Zojer, "A new gate drive technique for superjunction MOSFETs to compensate the effects of common source inductance," in *Applied Power Electronics Conference and Exposition (APEC), 2018 IEEE*, IEEE, pp. 2763–2768.